

BENCHMARK RESULTS FOR TESTING ADAPTIVE FINITE ELEMENT EIGENVALUE PROCEDURES

STEFANO GIANI, LUKA GRUBIŠIĆ, AND JEFFREY S. OVALL

ABSTRACT. A discontinuous Galerkin method, with hp -adaptivity based on the approximate solution of appropriate dual problems, is employed for highly-accurate eigenvalue computations on a collection of benchmark examples. After demonstrating the effectivity of our computed error estimates on a few well-studied examples, we present results for several examples in which the coefficients of the partial-differential operators are discontinuous. The problems considered here are put forward as benchmarks upon which other adaptive methods for computing eigenvalues may be tested, with results compared to our own.

1. INTRODUCTION

In 2005 Betcke and Treffethen wrote an influential paper [9] on the accurate computation of eigenvalues and eigenvectors of the Laplacian in planar regions, which gave insight into several interesting phenomena of the spectral theory of the Laplace operator on such domains. The computational approach used in [9] was a new implementation of the classical method of particular solutions. The structure of this method is such that it does not permit a similar analysis for other divergence-type elliptic operators whose coefficients are not C^∞ smooth. This class of problems includes many interesting multiphase examples such as photonic crystals and related problems, see [3, 26, 27] and in particular [18, Chapter 4]. A particular subclass of such problems are the so-called “jumping coefficient” problems for which the coefficients of the differential operators are piecewise smooth on some partition of the domain, but have jump discontinuities.

In the present work, we investigate a class of “jumping coefficient” problems using exponentially-convergent hp -adaptive discontinuous Galerkin (hp -DG) methods, with error estimates based on the Dual Weighted Residual (DWR) approach which has been already used successfully [15, 14] to study the stability of fluid dynamics problems. We argue that hp -adaptive methods are highly-efficient for computing eigenvalues of “jumping coefficient” problems — in terms of computational cost per accurate digit — and give indication of why we claim high accuracy of our computations. In many cases we discuss the significance (in terms of applications) of the models which our problems represent. We suggest that the eigenvalue approximations, convergence rates, effectivities of the computed error estimates, and computational cost information which we report here provide ideal benchmarks for study other adaptive finite element procedures designed to address such eigenvalue problems.

The model eigenvalue problem considered in this paper is:

$$(1.1) \quad Au := -\nabla \cdot (\mathcal{A}\nabla u) + Vu = \lambda u ,$$

2000 *Mathematics Subject Classification.* Primary: 65N30, Secondary: 65N25, 65N15.

Key words and phrases. eigenvalue problem, finite element method, a posteriori error estimates .

on a bounded domain $\Omega \subset \mathbb{R}^2$ and subject to a homogeneous Dirichlet boundary condition, i.e. $u = 0$ on $\partial\Omega$. Here, \mathbf{A} denotes the self-adjoint operator which is defined by this differential expression and we assume that the matrix-valued function \mathcal{A} is real symmetric and uniformly positive definite, i.e.

$$(1.2) \quad 0 < \underline{a} \leq \xi^T \mathcal{A}(x) \xi \leq \bar{a} \quad \text{for all } \xi \in \mathbb{R}^2 \quad \text{with } |\xi| = 1 \quad \text{and all } x \in \Omega .$$

The scalar potential V is real and bounded above and below by constants for all $x \in \Omega$, i.e.

$$(1.3) \quad 0 < \underline{V} \leq V(x) \leq \bar{V} \quad \text{for all } x \in \Omega .$$

The family of problems (1.1) is representative for a much larger class of singular stiff problems, see [23, 38], which can be written in the following abstract formulation, for $\kappa > 1$,

$$(1.4) \quad \mathbf{A}_\kappa u = \lambda u,$$

$$(1.5) \quad \mathfrak{h}_\kappa(u, v) = \mathfrak{h}_b(u, v) + \kappa \mathfrak{h}_e(u, v), \quad u, v \in \text{Dom}(\mathfrak{h}_b) \subset \text{Dom}(\mathfrak{h}_e).$$

Here we assume that the self-adjoint operator \mathbf{A}_κ is defined by positive definite quadratic forms \mathfrak{h}_κ , \mathfrak{h}_e and \mathfrak{h}_b in the sense of Kato [31], e.g. $(\mathbf{A}_\kappa^{1/2} u, \mathbf{A}_\kappa^{1/2} v)_{L^2} = \mathfrak{h}_\kappa(u, v)$, $u, v \in \text{Dom}(\mathfrak{h}_\kappa) = \text{Dom}(\mathbf{A}_\kappa^{1/2})$. In this setting we assume that \mathfrak{h}_e has a large null space in order for the problem to belong to the class of singular stiff problems. Problems with the structure (1.4)–(1.5) have applications in quantum mechanics, nano-optics, theory of vibrations of composite and porous materials and similar classes of singularly perturbed models. Furthermore, the differential expression (1.1) allows for a consideration of multi-scale eigenvalue problems for composite materials such as those from [12, 13]. More specifically, if $\mathcal{A}(x) = \mathcal{A}(x + \mathbf{k})$ and $V(x) = V(x + \mathbf{k})$ for all $\mathbf{k} \in \mathbb{Z}^2$ and $x \in \mathbb{R}^2$, one might consider the family of problems

$$(1.6) \quad \mathbf{A}_\varepsilon u := -\nabla \cdot (\mathcal{A}(\cdot/\varepsilon) \nabla u) + V(\cdot/\varepsilon) u = \lambda u ,$$

for $0 < \varepsilon \ll 1$.

Both classes of problems (1.4) and (1.6) converge to well-defined limit problems as $\kappa \rightarrow \infty$ or $\varepsilon \rightarrow 0$. Furthermore, the limit problems are frequently analytically soluble and posed only in a portion of the domain Ω . The computational challenge is to capture the transient behavior as the limiting procedure converges. In typical applications ε is small but nonzero and one is interested in capturing the oscillation and concentration properties of eigenvectors; whereas for large but finite κ one is often concerned with the tunneling properties, e.g. exhibiting exponential decay away from the domain where the limit problem is posed. One further difference between these problems is in the nature of the convergence. In the first case, we have that \mathbf{A}_κ^{-1} converges monotonically, which often leads to convergence of the resolvent in norm. In the second case we do not have monotonicity properties of the sequence $\mathbf{A}_\varepsilon^{-1}$ as $\varepsilon \rightarrow 0$, so at best we can conclude that the resolvents converge strongly. In its most general case strong resolvent convergence does not guarantee the conservation of multiplicities of eigenvalues in the passage to the limit (see [31]). Problems involving the operator \mathbf{A}_ε will not further be considered in this work; but we plan to return to this problem later, since the current state-of-the-art is to use numerical solutions on a very fine grid to test the convergence of a multi-scale numerical approximation method (cf. [12, Section 6] and [13]), and we believe that the approach put forth here has greater potential for efficiency.

The rest of the paper is structured as follows: In Section 2 we provide a detailed description of the *hp*-DG weak formulation of our model eigenvalue problem. Section 3 provides the background and basic results for the DWR error estimates which we employ. We describe,

in detail, two variants of the adaptive procedures used for our numerical experiments in Section 4. The bulk of the paper, Section 5, is devoted to presenting and discussing our benchmark results.

2. FORMULATION OF THE DISCONTINUOUS GALERKIN METHOD

In recent years the discontinuous Galerkin (DG) methods for elliptic problems [4] have become increasingly popular. Some of the main reasons for this increase of interest in DG methods is that allowing for discontinuities across elements gives extraordinary flexibility in terms of mesh design and choice of shape functions. Additionally, hp -DG, which are based on locally refined meshes and variable approximation orders, have been shown to achieve tremendous gains in computational efficiency for challenging problems [24, 25, 29, 28].

Since we are going to construct sequences of adaptively refined shape-regular meshes, we denote the meshes by \mathcal{T}_n , where n is the index of the mesh. The meshes \mathcal{T}_n are partitions of $\Omega \subset \mathbb{R}^2$ into open triangles or quadrilaterals $\{K\}_{K \in \mathcal{T}_n}$. We also assume that, in the interior of each element $K \in \mathcal{T}_n$, the positive definite matrix \mathcal{A} and the potential V are smooth. In presence of jumping coefficients, the jumps are aligned with the meshes used in this work. The diameter of an element $K \in \mathcal{T}_n$ is denoted by h_K . Due to our assumptions on the meshes, these diameters are of bounded variation, that is, there is a constant $b_1 \geq 1$ such that

$$(2.1) \quad b_1^{-1} \leq h_K/h_{K'} \leq b_1,$$

whenever K and K' share a common edge. We store the elemental diameters in the mesh size vector $\mathbf{h} = \{h_K : K \in \mathcal{T}_n\}$. Similarly, we associate with each element $K \in \mathcal{T}_n$ a polynomial degree $p_K \geq 1$ and define the degree vector $\mathbf{p} = \{p_K : K \in \mathcal{T}_n\}$. We assume that \mathbf{p} is of bounded variation as well, that is, there is a constant $b_2 \geq 1$ such that

$$(2.2) \quad b_2^{-1} \leq p_K/p_{K'} \leq b_2,$$

whenever K and K' share a common edge.

For a partition \mathcal{T}_n of Ω and a degree vector \mathbf{p} , we define the hp -version discontinuous Galerkin finite element space S_n of real valued functions by

$$(2.3) \quad S_n = \{v \in L^2(\Omega) : v|_K \in \mathcal{P}_{p_K}(K), K \in \mathcal{T}_n\},$$

where, if K is a triangle, $\mathcal{P}_{p_K}(K)$ is the space of polynomials on K of total degree less or equal p_K , otherwise if K is a quadrilateral, $\mathcal{P}_{p_K}(K)$ is the space of polynomials on K of degree less or equal p_K in each dimension.

Next, we define some trace operators that are required for the DG methods. To this end, we denote by $\mathcal{E}_{\mathcal{I}}(\mathcal{T}_n)$ the set of all interior edges of the partition \mathcal{T}_n of Ω , and by $\mathcal{E}_{\Gamma}(\mathcal{T}_n)$ the set of all boundary edges of \mathcal{T}_n . Furthermore, we define $\mathcal{E}(\mathcal{T}_n) = \mathcal{E}_{\mathcal{I}}(\mathcal{T}_n) \cup \mathcal{E}_{\Gamma}(\mathcal{T}_n)$. The boundary ∂K of an element K and the sets $\partial K \setminus \Gamma$ and $\partial K \cap \Gamma$ will be identified in a natural way with the corresponding subsets of $\mathcal{E}(\mathcal{T}_n)$.

Let K^+ and K^- be two adjacent elements of \mathcal{T}_n , and $\kappa \in \mathcal{E}_{\mathcal{I}}(\mathcal{T}_n)$ given by $\kappa = \partial K^+ \cap \partial K^-$. Furthermore, let v be a complex scalar-valued function, that is smooth inside each element K^{\pm} . By v^{\pm} , we denote the traces of v on κ taken from within the interior of K^{\pm} , respectively. Then, since we are dealing with jumping coefficients we need to use the

definition of the weighted average of the diffusive flux $\mathcal{A}\nabla_n v$ along $\kappa \in \mathcal{E}_{\mathcal{I}}(\mathcal{T}_n)$ introduced in [20]

$$\{\{\mathcal{A}\nabla_n v\}\} = \omega^-(\mathcal{A}\nabla_n v)^- + \omega^+(\mathcal{A}\nabla_n v)^+,$$

where

$$\omega^- = \frac{\mathbf{n}_{K^+}^t \mathcal{A}^+ \mathbf{n}_{K^+}}{\mathbf{n}_{K^-}^t \mathcal{A}^- \mathbf{n}_{K^-} + \mathbf{n}_{K^+}^t \mathcal{A}^+ \mathbf{n}_{K^+}}, \quad \omega^+ = \frac{\mathbf{n}_{K^-}^t \mathcal{A}^- \mathbf{n}_{K^-}}{\mathbf{n}_{K^-}^t \mathcal{A}^- \mathbf{n}_{K^-} + \mathbf{n}_{K^+}^t \mathcal{A}^+ \mathbf{n}_{K^+}},$$

where we denote by \mathbf{n}_{K^\pm} the unit outward normal vector of ∂K^\pm , respectively. Similarly, for a scalar function we have the following weighted average

$$\{\{v\}\} = \omega^- v^+ + \omega^+ v^-.$$

Then, the jump of v across $\kappa \in \mathcal{E}_{\mathcal{I}}(\mathcal{T}_n)$ is given by

$$[[v]] = v^+ \mathbf{n}_{K^+} + v^- \mathbf{n}_{K^-},$$

$$[[\mathcal{A}\nabla_n v]] = \mathcal{A}_{K^+} \nabla_n v^+ \cdot \mathbf{n}_{K^+} + \mathcal{A}_{K^-} \nabla_n v^- \cdot \mathbf{n}_{K^-}.$$

On a boundary edge $\kappa \in \mathcal{E}_{\Gamma}(\mathcal{T}_n)$, we set $\{\{\mathcal{A}\nabla_n v\}\} = \mathcal{A}\nabla_n v$ and $[[v]] = v \mathbf{n}$, with \mathbf{n} denoting the unit outward normal vector on the boundary Γ .

For a mesh \mathcal{T}_n on Ω and a polynomial degree vector \mathbf{p} , let S_n be the hp -version finite element space defined in (2.3). We consider the (symmetric) weighted interior penalty discretization [20] of (1.1): find $(\lambda_n, u_n) \in \mathbb{R} \times S_n$ such that

$$(2.4) \quad A_n(u_n, v) = \lambda_n(u_n, v), \quad \text{for all } v \in S_n,$$

with $(u_n, u_n) = 1$ and where

$$\begin{aligned} A_n(u, v) &:= \sum_{K \in \mathcal{T}_n} \int_K \mathcal{A}_K \nabla_n u \cdot \nabla_n v + V u v \, d\mathbf{r} \\ &\quad - \sum_{\kappa \in \mathcal{E}(\mathcal{T}_n)} \int_{\kappa} (\{\{\mathcal{A}\nabla_n v\}\} \cdot [u] + \{\{\mathcal{A}\nabla_n u\}\} \cdot [v]) \, ds + \sum_{\kappa \in \mathcal{E}(\mathcal{T}_n)} \int_{\kappa} \mathbf{c} [u] \cdot [v] \, ds, \\ (u, v) &:= \int_{\Omega} u v \, d\mathbf{r}, \end{aligned}$$

here, ∇_n denotes the element wise gradient operator and \mathcal{A}_K denotes the restriction of \mathcal{A}_K onto K . Furthermore, the function $\mathbf{c} \in L^\infty(\mathcal{E}(\mathcal{T}_n))$ is the discontinuity stabilisation function that is chosen as follows: we define the functions $\mathbf{h} \in L^\infty(\mathcal{E}(\mathcal{T}_n))$ and $\mathbf{p} \in L^\infty(\mathcal{E}(\mathcal{T}_n))$ by

$$\mathbf{h}(\mathbf{r}) := \begin{cases} \min(h_{K^+}, h_{K^-}), & \mathbf{r} \in \kappa \in \mathcal{E}_{\mathcal{I}}(\mathcal{T}_n), \kappa = \partial K^+ \cap \partial K^-, \\ h_K, & \mathbf{r} \in \kappa \in \mathcal{E}_{\Gamma}(\mathcal{T}_n), \kappa \in \partial K \cap \Gamma, \end{cases}$$

$$\mathbf{p}(\mathbf{r}) := \begin{cases} \max(p_{K^+}, p_{K^-}), & \mathbf{r} \in \kappa \in \mathcal{E}_{\mathcal{I}}(\mathcal{T}_n), \kappa = \partial K^+ \cap \partial K^-, \\ p_K, & \mathbf{r} \in \kappa \in \mathcal{E}_{\Gamma}(\mathcal{T}_n), \kappa \in \partial K \cap \Gamma, \end{cases}$$

and set the penalty parameter to be

$$(2.5) \quad \mathbf{c} = \gamma \omega^+ \mathbf{n}_{K^+}^t \mathcal{A}^+ \mathbf{n}_{K^+} + \frac{\mathbf{p}^2}{\mathbf{h}},$$

with a parameter $\gamma > 0$ that is independent of \mathbf{h} , \mathbf{p} , \mathcal{A}_{K^+} and \mathcal{A}_{K^-} . The parameter \mathbf{c} defined here is an hp -version of the weighted penalty parameter [20].

3. GOAL-ORIENTED A POSTERIORI ERROR ESTIMATION

In this section we introduce the *a posteriori* analysis, which is based on an auxiliary problem described below. The actual form of the auxiliary problem depends on the goal functional $J(\cdot)$ utilized. We note that, even if the primal problem (1.1) is non-linear, the auxiliary problem, which is related to the dual/adjoint operator in (1.1), is linear for our choice of $J(\cdot)$. The advantages of this approach are mainly two: effectivity and flexibility. As can be seen in Section 5, the *a posteriori* error estimator gives a very precise estimation of the true error. Moreover, the analysis can be easily used with different goal functional to obtain an automatic adaptive method to target particular measurements of the error. In this section we consider only a functional to estimate the error for eigenvalues.

The analysis in this section is only for eigenvalue problems of the form (1.1) whose eigenfunctions u are sufficiently smooth: u is continuous, and $\mathcal{A}\nabla u \in [H^1(\Omega)]^2$. This type of additional regularity assumption is not uncommon in *a priori* or *a posteriori* error analysis for jumping coefficient problems, and can be found, for example, in [36, Theorem 4.11], the main approximation result in that work. For a recent *a priori* analysis see [39]. To this end we introduce the notation $H_{\mathcal{A}}^2(\Omega) := \{v \in L^2(\Omega) : \mathcal{A}\nabla v \in [H^1(\Omega)]^2\}$. In the case that $\mathcal{A} \equiv 1$ everywhere the definition of $H_{\mathcal{A}}^2(\Omega)$ coincides with the standard $H^2(\Omega)$. More generally the condition $u \in H_{\mathcal{A}}^2(\Omega)$ is satisfied by all eigenfunctions when Ω is convex and when the interfaces between discontinuous values of \mathcal{A} are smooth. However, we will demonstrate in Section 5 that the goal-oriented error estimator performs well also when the eigenfunctions are not in $H_{\mathcal{A}}^2(\Omega)$.

In order to proceed we recast the discrete problem (2.4) in a more suitable, but equivalent form: *seek eigenpairs* $\hat{u}_n := (\lambda_n, u_n) \in \mathbb{R} \times S_n$, *such that*

$$\mathcal{N}(\hat{u}_n, \hat{v}_n) = 0 \quad \forall \hat{v}_n = (\delta_n, v_n) \in \mathbb{R} \times S_n ,$$

where

$$(3.1) \quad \mathcal{N}(\hat{u}_n, \hat{v}_n) := -A_n(u_n, v_n) + \lambda_n(u_n, v_n) + \delta_n(\|u_n\|_0^2 - 1) ,$$

where $\|\cdot\|_0$ is the standard $L^2(\Omega)$ norm.

Now, we briefly outline the key steps involved in estimating the error in the goal functional $J(\hat{u}) - J(\hat{u}_n)$ employing the Dual Weighted Residual (DWR) technique (cf. [7]), for a general target functional of practical interest $J(\cdot)$. The same analysis can be reused with different goal functionals, leading to different auxiliary problems to be solved. In order to show the flexibility of the DWR technique, we introduce the actual definition of the functional $J(\cdot)$ used in the numerics only later in this section. For the moment we work with a general $J(\cdot)$ which is assumed to be differentiable. So, we write $\bar{J}(\cdot, \cdot; \cdot)$ to denote the mean value linearization of $J(\cdot)$, defined by

$$\bar{J}(\hat{u}, \hat{u}_n; \hat{u} - \hat{u}_n) = J(\hat{u}) - J(\hat{u}_n) = \int_0^1 J'[\theta\hat{u} + (1-\theta)\hat{u}_n](\hat{u} - \hat{u}_n) d\theta ,$$

where $J'[\hat{w}](\cdot)$ denotes the Fréchet derivative of $J(\cdot)$ evaluated at some $\hat{w} \in \mathbb{R} \times S$, and $S := S_n + H_{\mathcal{A}}^2(\Omega)$ is the space of functions that are sum of a finite element function in S_n and a function in $H_{\mathcal{A}}^2(\Omega)$. In the same way, we write

$$\mathcal{M}(\hat{u}, \hat{u}_n; \hat{u} - \hat{u}_n, \hat{w}) = \mathcal{N}(\hat{u}, \hat{w}) - \mathcal{N}(\hat{u}_n, \hat{w}) = \int_0^1 \mathcal{N}'_{\hat{u}}[\theta\hat{u} + (1-\theta)\hat{u}_n](\hat{u} - \hat{u}_n, \hat{w}) d\theta .$$

We now introduce the following formal dual problem: find $\hat{z} \in \mathbb{R} \times S$ such that

$$(3.2) \quad \mathcal{M}(\hat{u}, \hat{u}_n; \hat{w}, \hat{z}) = \bar{J}(\hat{u}, \hat{u}_n; \hat{w}) , \quad \forall \hat{w} \in \mathbb{R} \times S .$$

We assume that (3.2) possesses a unique solution. This assumption is, of course, dependent on both the definition of $\mathcal{M}(\hat{u}, \hat{u}_n; \cdot, \cdot)$ and the target functional under consideration. For the proceeding error analysis, we must therefore assume that (3.2) is well-posed. In order to compute our error estimator we are not going to solve (3.2), but compute a discrete approximation of it in order to obtain an accurate approximation of the dual solution \hat{z} .

The next theorem introduce the residual forming the error estimator and its corollary introduce a simple way to compute an upper bound of the error.

Lemma 3.1. *Let $\hat{u} \in \mathbb{R} \times H_{\mathcal{A}}^2(\Omega)$ be an eigenpair of (1.1), then for any $\hat{z} \in \mathbb{R} \times S$ we have*

$$\mathcal{N}(\hat{u}, \hat{z}) = 0 .$$

Proof. Without loss of generality we assume that $\hat{z} := (\delta, z_n + z_c)$, with $\delta \in \mathbb{R}$, $z_n \in S_n$ and $z_c \in H_{\mathcal{A}}^2(\Omega)$. Applying (3.1) we have

$$(3.3) \quad \mathcal{N}(\hat{u}, \hat{z}) = -A_n(u, z_n + z_c) + \lambda(u, z_n + z_c) = -A_n(u, z_n) + \lambda(u, z_n) - A_n(u, z_c) + \lambda(u, z_c) .$$

Because u is continuous and $\mathcal{A}\nabla_n u$ is continuous across the faces of the mesh we have by integration-by-parts that

$$(3.4) \quad \begin{aligned} A_n(u, z_n) &= \sum_{K \in \mathcal{T}_n} \int_K \mathcal{A}_K \nabla_n u \cdot \nabla_n z_n + V u z_n \, d\mathbf{r} - \sum_{\kappa \in \mathcal{E}(\mathcal{T}_n)} \int_{\kappa} \{\{\mathcal{A}\nabla_n u\}\} \cdot \llbracket z_n \rrbracket \, ds \\ &= \int_{\Omega} -\nabla \cdot (\mathcal{A}\nabla u) z_n + V u z_n \, dx = \lambda(u, z_n) . \end{aligned}$$

Similarly because z_c is continuous we have by integration-by-parts:

$$(3.5) \quad A_n(u, z_c) = \sum_{K \in \mathcal{T}_n} \int_K \mathcal{A}_K \nabla_n u \cdot \nabla_n z_c + V u z_c \, d\mathbf{r} = \lambda(u, z_c) .$$

Substituting (3.4) and (3.5) into (3.3) we have the result. Q.E.D.

Theorem 3.2. *Let us denote by \hat{z}_n the finite element approximation of \hat{z} in S_n . Then*

$$J(\hat{u}) - J(\hat{u}_n) = -\mathcal{N}(\hat{u}_n, \hat{z} - \hat{z}_n) = \sum_{K \in \mathcal{T}_n} \eta_K , \quad \forall \hat{z}_n \in \mathbb{R} \times S_n ,$$

where the residual η_K is defined as:

$$\begin{aligned} \eta_K &= \int_K -(\lambda_n u_n + \nabla \cdot (\mathcal{A}_K \nabla u_n) - V u_n)(z - z_n) \\ &\quad - \frac{1}{2} \int_{\partial K/\Gamma} \{\{\mathcal{A}\nabla(z - z_n)\}\} \cdot \llbracket u_n \rrbracket + \frac{1}{2} \int_{\partial K/\Gamma} \llbracket \mathcal{A}\nabla u_n \rrbracket \{\{z - z_n\}\} \\ &\quad + \frac{1}{2} \int_{\partial K/\Gamma} c \llbracket u_n \rrbracket \llbracket z - z_n \rrbracket - \int_{\partial K \cap \Gamma} \mathcal{A}_K \frac{\partial(z - z_n)}{\partial \mathbf{n}} u_n + \int_{\partial K \cap \Gamma} c u_n (z - z_n) . \end{aligned}$$

Proof. From the formal dual problem (3.2) and by Lemma 3.1 we have that:

$$\begin{aligned} J(\hat{u}) - J(\hat{u}_n) &= \bar{J}(\hat{u}, \hat{u}_n; \hat{u} - \hat{u}_n) = \mathcal{M}(\hat{u}, \hat{u}_n; \hat{u} - \hat{u}_n, \hat{z}) \\ &= \mathcal{N}(\hat{u}, \hat{z}) - \mathcal{N}(\hat{u}_n, \hat{z}) = -\mathcal{N}(\hat{u}_n, \hat{z} - \hat{z}_n), \end{aligned}$$

where in the last equality we used the fact that $\mathcal{N}(\hat{u}_n, \hat{z}_n) = 0$. Then by the definition of $A_n(\cdot, \cdot)$ and since $\|u_n\|_0 = 1$ we have:

$$\begin{aligned} -\mathcal{N}(\hat{u}_n, \hat{z} - \hat{z}_n) &= A_n(\hat{u}_n, z - z_n) - \lambda_n b(u_n, z - z_n) \\ &= \sum_{K \in \mathcal{T}_n} \int_K \mathcal{A}_K \nabla_n u_n \cdot \nabla_n (z - z_n) + V u_n (z - z_n) \, d\mathbf{r} \\ &\quad - \sum_{\kappa \in \mathcal{E}(\mathcal{T}_n)} \int_{\kappa} (\{\{\mathcal{A} \nabla_n (z - z_n)\}\} \cdot \llbracket u_n \rrbracket + \{\{\mathcal{A} \nabla_n u_n\}\} \cdot \llbracket z - z_n \rrbracket) \, ds \\ &\quad + \sum_{\kappa \in \mathcal{E}(\mathcal{T}_n)} \int_{\kappa} \mathbf{c} \llbracket u_n \rrbracket \cdot \llbracket z - z_n \rrbracket \, ds. \end{aligned}$$

Integrating by parts the second order term elementwise we obtain:

$$\begin{aligned} \sum_{K \in \mathcal{T}_n} \int_K \mathcal{A}_K \nabla_n u_n \cdot \nabla_n (z - z_n) \, d\mathbf{r} &= \sum_{K \in \mathcal{T}_n} \left\{ \int_K -\nabla_n \cdot (\mathcal{A}_K \nabla_n u_n) (z - z_n) \, d\mathbf{r} \right. \\ &\quad \left. + \int_{\partial K} \mathcal{A}_K \frac{\partial u_n}{\partial \mathbf{n}_{K^+}} (z - z_n) \, ds \right\} \end{aligned}$$

The second term on the right hand side can then further be expanded like

$$\begin{aligned} \sum_{K \in \mathcal{T}_n} \int_{\partial K} \mathcal{A}_K \frac{\partial u_n}{\partial \mathbf{n}_{K^+}} (z - z_n) \, ds &= \sum_{\kappa \in \mathcal{E}_{\mathcal{I}}(\mathcal{T}_n)} \int_{\kappa} \{\{\mathcal{A} \nabla u_n\}\} \cdot \llbracket z - z_n \rrbracket + \llbracket \mathcal{A} \nabla u_n \rrbracket \cdot \{\{z - z_n\}\} \, ds \\ &\quad + \sum_{\kappa \in \mathcal{E}_{\Gamma}(\mathcal{T}_n)} \int_{\kappa} \mathcal{A} \frac{\partial u_n}{\partial \mathbf{n}} (z - z_n) \, ds. \end{aligned}$$

Then substituting this back we finally obtain:

$$\begin{aligned}
-\mathcal{N}(\hat{u}_n, \hat{z} - \hat{z}_n) &= \sum_{K \in \mathcal{T}_n} \int_K (-\nabla \cdot (\mathcal{A}_K \nabla u_n) + V u_n - \lambda_n u_n)(z - z_n) \, d\mathbf{r} \\
&\quad - \sum_{\kappa \in \mathcal{E}_{\mathcal{I}}(\mathcal{T}_n)} \int_{\kappa} \{\{\mathcal{A} \nabla_n(z - z_n)\}\} \cdot \llbracket u_n \rrbracket \, ds + \sum_{\kappa \in \mathcal{E}_{\mathcal{I}}(\mathcal{T}_n)} \int_{\kappa} \llbracket \mathcal{A} \nabla u_n \rrbracket \{\{z - z_n\}\} \, ds \\
&\quad + \sum_{\kappa \in \mathcal{E}_{\mathcal{I}}(\mathcal{T}_n)} \int_{\kappa} \mathbf{c} \llbracket u_n \rrbracket \cdot \llbracket z - z_n \rrbracket \, ds - \sum_{\kappa \in \mathcal{E}_{\Gamma}(\mathcal{T}_n)} \int_{\kappa} \mathcal{A} \frac{\partial(z - z_n)}{\partial \mathbf{n}} u_n \, ds \\
&\quad + \sum_{\kappa \in \mathcal{E}_{\Gamma}(\mathcal{T}_n)} \int_{\kappa} \mathbf{c} u_n (z - z_n) \, ds ,
\end{aligned}$$

which is equivalent to $\sum_{K \in \mathcal{T}_n} \eta_K$. Q.E.D.

Corollary 3.3. *Under the same assumptions as in Theorem 3.2 we have:*

$$|J(\hat{u}) - J(\hat{u}_n)| \leq \sum_{K \in \mathcal{T}_n} |\eta_K|$$

Proof. The result can be easily proved from Theorem 3.2 using the triangle inequality. Q.E.D.

With Theorem 3.2 in mind, we introduce the non-linear functional of interest to estimate and target with the hp -adaptive method the error in a given eigenvalue λ of interest. This leads us to a specific auxiliary problem to be solved in order to compute a good approximation of the dual solution \hat{z} to substitute back in the residuals of Theorem 3.2. It is important to note that, even if the form of the residuals of Theorem 3.2 remain unchanged, the result holds for different functional of interests because the auxiliary problem, and so the dual solution \hat{z} , are dependent on the definition of $J(\cdot)$. In other words the dual solution \hat{z} works as a sensitivity parameter in the residuals, to finely tune them to target a specific measurement of the error. The functional of interest may be defined by

$$(3.6) \quad J(\hat{v}) := \delta \|v\|_0^2 ,$$

where $\hat{v} := (\delta, v)$. In which case

$$J(\hat{u}) - J(\hat{u}_n) = \lambda - \lambda_n ,$$

since that $\|u\|_0 = \|u_n\|_0 = 1$. Then we use the definition of $J(\cdot)$ (3.6) to write down explicitly the Fréchet derivative of $J(\cdot)$ and of $\mathcal{N}(\cdot, \cdot)$ at \hat{u} :

$$J'[\hat{u}](\hat{v}) := 2\lambda(u, v) + \delta \|u\|_0^2 ,$$

and

$$\mathcal{N}'[\hat{u}](\hat{v}, \hat{z}) := A_n(v, z) - \lambda(v, z) - \delta(u, z) + 2\beta(u, v) ,$$

with $\hat{v} := (\delta, v)$ and $\hat{z} := (\beta, z)$. Since \hat{u} is unavailable, we introduce an auxiliary problem, which is an approximation of problem (3.2) that is based on the linearization about \hat{u}_n rather than $\hat{u} - \hat{u}_n$:

$$(3.7) \quad \mathcal{N}'[\hat{u}_n](\hat{v}, \hat{z}) = J'[\hat{u}_n](\hat{v}) .$$

This leads to the following linear problem, which has a unique solution: seek $\hat{z} := (\beta, z) \in \mathbb{R} \times S$, such that

$$A_n(v, z) - \lambda_n(v, z) - \delta(u_n, z) + 2\beta(u_n, v) = 2\lambda_n(u_n, v) + \delta\|u_n\|_0^2,$$

for all $(\delta, v) \in \mathbb{R} \times S$.

It should be clear from the definition of η_K in Theorem 3.2 that these quantities are not explicitly computable, in general. In order to obtain a computable quantity, the dual solution \hat{z} must be approximated in some suitable finite element space. Apparently the approximation $z_n \in S_n$ is of no use, because $\mathcal{N}(\hat{u}_n, \hat{z}_n - z_n) = 0$. In practice, it is necessary to compute an approximation of z in a space \tilde{S}_n which is “richer” than S_n . Two natural choices are constructed from S_n as follows:

- (1) Maintain the same partition, but increase the local polynomial degree by one on each element.
- (2) Adaptively refine the partition \mathcal{T}_n and the local polynomial degrees on each element.

Obviously, there are many variations on this theme, but, in the present work, we employ either of the options above, depending on the regularity of dual solution. Our adaptive algorithms are described in detail in the following section.

Remark 3.4. In what follows, we will abuse notation slightly by using η_K to denote our computed approximations of the ideal quantities η_K defined in Theorem 3.2.

Remark 3.5. Let us note that the main result on which we based our analysis is the error representation result of Theorem 3.2. In fact based on this we will propose in Section 5 the use of $\lambda_n + \sum_{K \in \mathcal{T}_n} \eta_K$ as an improved approximation of λ (under some additional assumptions). For this reason we will be using the quantity $|\sum_{K \in \mathcal{T}_n} \eta_K|$ for error control, rather than $\sum_{K \in \mathcal{T}_n} |\eta_K|$ as suggested by Corollary 3.3.

4. OUR ADAPTIVE ALGORITHMS

The *hp*-adaptive algorithms used for the numerical experiments in Section 5 are expressed below in Algorithm 1 and Algorithm 2. The difference between these algorithms is reflected in the space \tilde{S}_n in which the dual solution is approximated, as briefly discussed in Section 3. We will see later that, although both algorithms yield essentially the same convergence rates for the eigenvalue errors, Algorithm 2 is sometimes necessary for achieving effectivities—the ratio of true and estimated errors—near 1. In situations where the effectivity is near 1, we will see that the computed error estimates can be automatically “recycled” in order to accelerate convergence.

Algorithm 1 Goal-oriented adaptive algorithm, Version 1

$(\lambda_{j,n}, u_{j,n}, \mathcal{T}_{j,n}, S_n) := \text{GoalDG}(\mathcal{T}_0, S_0, j, \theta, \text{tol}, J(\cdot))$
 $n = 0$
repeat
 Compute the j -th eigenpair $(\lambda_{j,n}, u_{j,n})$ on \mathcal{T}_n
 $(\tilde{\mathcal{T}}_n, \tilde{S}_n) := \text{DualSpace}(\mathcal{T}_n, S_n)$
 Compute $(\tilde{\delta}_n, \tilde{z}_n) \in \mathbb{R} \times \tilde{S}_n$ solving the linear problem (3.7) on $\tilde{\mathcal{T}}_n$
 Compute η_K for all $K \in \mathcal{T}_n$
 if $|\sum_{K \in \mathcal{T}_n} \eta_K| < \text{tol}$ **then**
 exit
 else
 $(\mathcal{T}_{n+1}, S_{n+1}) := \text{Refine}(\mathcal{T}_n, S_n, \theta, \eta)$
 $n = n + 1$
 end if
until

Algorithm 2 Goal-oriented adaptive algorithm, Version 2

$(\lambda_{j,n}, u_{j,n}, \mathcal{T}_{j,n}, S_n) := \text{GoalDGAdapt}(\mathcal{T}_0, S_0, j, \theta, \text{tol}, J(\cdot), m)$
 $n = 0$
repeat
 Compute the j -th eigenpair $(\lambda_{j,n}, u_{j,n})$ on \mathcal{T}_n
 $(\tilde{\mathcal{T}}_n, \tilde{S}_n) := \text{DualSpaceAdapt}(\mathcal{T}_n, S_n, m)$
 Compute $(\tilde{\delta}_n, \tilde{z}_n) \in \mathbb{R} \times \tilde{S}_n$ solving the linear problem (3.7) on $\tilde{\mathcal{T}}_n$
 Compute η_K for all $K \in \mathcal{T}_n$
 if $|\sum_{K \in \mathcal{T}_n} \eta_K| < \text{tol}$ **then**
 exit
 else
 $(\mathcal{T}_{n+1}, S_{n+1}) := \text{Refine}(\mathcal{T}_n, S_n, \theta, \eta)$
 $n = n + 1$
 end if
until

Both algorithms take as input: an initial mesh \mathcal{T}_0 , an initial DG space S_0 , the index j of the eigenpair to approximate, a real value $0 \leq \theta \leq 1$ to tune the marking strategy, a real and positive value tol which prescribes the required tolerance, and finally the goal functional $J(\cdot)$ that should be used. Algorithm 2 requires an additional parameter $m > 0$ that fixes the number of adaptive refinement steps which may be used in the construction of the dual mesh for \tilde{S}_n . The algorithms have a very simple structure that consists of a repeat-until loop. During each iteration of the loop a new approximation of the eigenpair of interest is computed, then the finer space \tilde{S}_n is constructed and an approximate solution $(\tilde{\delta}_n, \tilde{z}_n)$ of problem (3.7) is computed. Finally the error estimator is calculated and, if the estimated error $|\sum_{K \in \mathcal{T}_n} \eta_K|$ is lower than the prescribed tolerance tol the algorithm stops; otherwise the mesh \mathcal{T}_n and the space S_n are refined and another iteration follows. To complete the

description of the algorithms we must describe the functions DualSpace, DualSpaceAdapt and Refine.

The function Refine applies a simple fixed-fraction strategy to mark a minimal subset of elements containing a portion of the error proportional to θ . Then the choice for each marked element between splitting the element into smaller elements (h -refinement) or increasing the polynomial order (p -refinement) is made by testing the local analyticity of the solution in the interior of the element as described in [19, 30]. The function DualSpace sets $\tilde{\mathcal{T}}_n \equiv \mathcal{T}_n$ and constructs the space \tilde{S}_n by increasing by 1 the order of polynomials in each element in S_n .

For Algorithm 2, in order to construct the dual space \tilde{S}_n , the routine DualSpaceAdapt uses the energy norm error estimator $\tilde{\eta}$:

$$\tilde{\eta}^2 = \sum_{K \in \mathcal{T}_h} \tilde{\eta}_K^2 ,$$

where $\tilde{\eta}_K$ is an indicator of the error on the element K . The terms $\tilde{\eta}_K$ are defined as follows:

$$\tilde{\eta}_K^2 = \tilde{\eta}_{R_K}^2 + \tilde{\eta}_{F_K}^2 + \tilde{\eta}_{J_K}^2 ,$$

where

$$\begin{aligned} \tilde{\eta}_{R_K}^2 &= p_K^{-2} h_K^2 \|\tilde{\delta}_n + \nabla \cdot (\mathcal{A} \nabla \tilde{z}_n)\|_{0,K}^2 , \\ \tilde{\eta}_{F_K}^2 &= \frac{1}{2} \sum_{\kappa \in \mathcal{E}_{\mathcal{I}}} p^{-1} \mathbf{h} \|\llbracket \mathcal{A} \nabla \tilde{z}_n \rrbracket\|_{0,\kappa}^2 , \\ \tilde{\eta}_{J_K}^2 &= \frac{1}{2} \sum_{\kappa \in \mathcal{E}_{\mathcal{I}}} \mathbf{c} \|\llbracket \tilde{z}_n \rrbracket\|_{0,\kappa}^2 + \sum_{\kappa \in \mathcal{E}_{\Gamma}} \mathbf{c} \|\llbracket \tilde{z}_n \rrbracket\|_{0,\kappa}^2 . \end{aligned}$$

Similar error estimators have been used in [40, 43], where they are seen to lead to exponential convergence rates for both smooth and non-smooth problems. Algorithm 3 outlines how the routine DualSpaceAdapt works.

Algorithm 3 Adaptive dual space construction

$(\tilde{\mathcal{T}}_n, \tilde{S}_n) = \text{DualSpaceAdapt}(\mathcal{T}_n, S_n, m)$

$r = 0$

$\tilde{\mathcal{T}}_r = \mathcal{T}_n$

$\tilde{S}_r = S_n$

repeat

 Compute $(\tilde{\delta}_r, \tilde{z}_r) \in \mathbb{R} \times \tilde{S}_r$ solving the linear problem (3.7) on $\tilde{\mathcal{T}}_r$

 Compute $\tilde{\eta}_K$ for all $K \in \tilde{\mathcal{T}}_r$

$(\tilde{\mathcal{T}}_{r+1}, \tilde{S}_{r+1}) = \text{Refine}(\tilde{\mathcal{T}}_r, \tilde{S}_r, \theta, \tilde{\eta})$

$r = r + 1$

until $r < m$

$\tilde{\mathcal{T}}_n = \tilde{\mathcal{T}}_r$

$\tilde{S}_n = \tilde{S}_r$

5. BENCHMARKS

All experiments in this section have been performed using AptoFEM (www.aptofem.com) on a single processor desktop machine. This code uses ARPACK to compute the (algebraic) eigenvalues and MUMPS to solve linear systems. This section is organized in several subsections which illustrate various characteristics of our approach on a variety of problems.

5.1. Basic Illustrations for the Laplacian on the Unit Square. We illustrate some of the basic features of our approach, and introduce terminology used for other experiments, on the following simple problem: *Find eigenpairs* $(\lambda, u) \in \mathbb{R} \times H_0^1(\Omega)$ *such that* $\|u\|_0 = 1$, *where*

$$(5.1) \quad \begin{cases} -\Delta u = \lambda u, & \text{in } \Omega, \\ u = 0, & \text{on } \partial\Omega. \end{cases}$$

Here, $\Omega = (0, 1)^2$ is the unit square. Because the eigenvalues and eigenfunctions (which are analytic) are known explicitly, $\lambda_{ij} = (i^2 + j^2)\pi$ and $u_{ij} = \sin(i\pi x)\sin(j\pi y)$, it is trivial to check certain properties of our estimator and adaptive scheme. This indicates how our approach might be expected to perform in such ideal cases—although we will see that similar performance is achieved in low-regularity situations as well.

In Table 1 and Table 2 we have used Algorithm 1 to compute the first and the second eigenvalues. We note that the second eigenvalue $5\pi^2$ is degenerate—its corresponding invariant subspace has dimension 2. The column DOFs contains the number of degrees of freedom in the finite element space S_n and the column elements contains the number of elements in the mesh \mathcal{T}_n . The last column contains the effectivity index which is defined as $|\lambda - \lambda_n| / |\sum_{K \in \mathcal{T}_n} \eta_K|$, which we see is very close to 1 even for our coarsest problems. In Figure 1 we plot $|\lambda - \lambda_n|$ versus DOFs, and, as can be seen, the two graphs suggest exponential convergence rate. The exceptional effectivity of the error estimator, and its apparent utility in guiding adaptive refinement, have been seen in other contexts as well (for example, fluid-dynamic problems in [22]), suggesting that functional error estimation and goal-oriented of this sort can have broad applicability.

n	DOFs	elements	$ \lambda - \lambda_n $	$\sum_{K \in \mathcal{T}_n} \eta_K$	effectivity
1	192	32	5.030e-02	4.984e-02	1.01
2	224	32	2.658e-02	2.605e-02	1.02
3	264	32	1.728e-02	1.690e-02	1.02
4	320	32	6.080e-04	6.032e-04	1.01
5	360	32	3.067e-04	3.020e-04	1.02
6	420	32	1.480e-04	1.444e-04	1.03
7	480	32	4.596e-06	4.574e-06	1.00
8	528	32	2.361e-06	2.338e-06	1.01
9	588	32	1.684e-06	1.665e-06	1.01
10	672	32	2.363e-08	2.355e-08	1.00
11	728	32	1.189e-08	1.180e-08	1.01
12	812	32	3.043e-09	2.989e-09	1.02

TABLE 1. Results for the hp -adaptive method on the first eigenvalue $\lambda = 2\pi^2$.

n	DOFs	elements	$ \lambda - \lambda_n $	$\sum_{K \in \mathcal{T}_n} \eta_K$	effectivity
1	192	32	4.121e-01	4.020e-01	1.03
2	254	35	1.825e-01	1.751e-01	1.04
3	356	50	1.245e-01	1.188e-01	1.05
4	502	65	2.231e-02	2.210e-02	1.01
5	620	65	6.655e-03	6.509e-03	1.02
6	734	65	1.375e-03	1.359e-03	1.01
7	1054	86	1.332e-04	1.318e-04	1.01
8	1207	86	2.480e-05	2.404e-05	1.03
9	1328	86	2.139e-06	2.123e-06	1.01
10	1632	86	1.580e-07	1.577e-07	1.00
11	1818	86	1.998e-08	1.984e-08	1.01
12	2157	86	5.559e-10	5.558e-10	1.00

TABLE 2. Results for the hp -adaptive method on the eigenvalue $\lambda = 5\pi^2$.

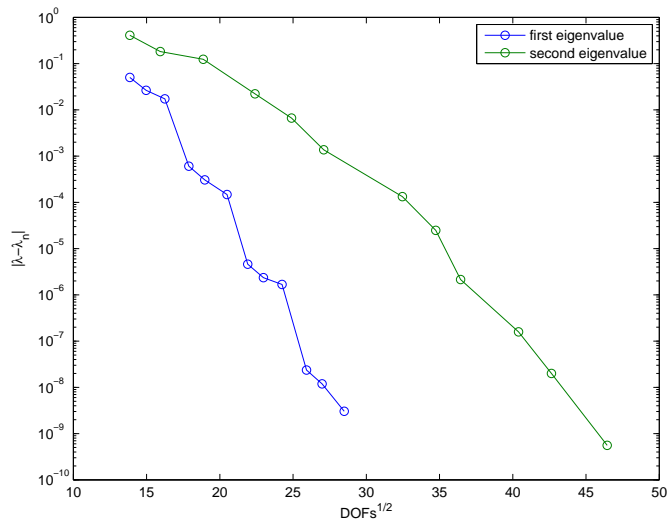


FIGURE 1. Convergence of the first two eigenvalues for the Dirichlet Laplacian on the unit square.

In situation such as that above, in which the effectivity of the estimator is near 1, Theorem 3.2 automatically suggests that $\lambda_n + \sum_{K \in \mathcal{T}_n} \eta_K$ is a better approximation of λ than is λ_n . This heuristic is validated in Tables 3-4, where we see decreases in error by one or two orders of magnitude! The principle of augmenting a computed eigenvalue with a highly-accurate error estimate is seen in other methods as well. In [35], the authors use gradient recovery techniques to improve their eigenvalue computations, and in [6] hierarchical basis techniques are used for the same purpose; in both cases, the approximation spaces S_n were continuous Lagrange elements of degree 1. Such “acceleration” procedures belong to a larger class of post-processing techniques, such as those used in [37, 42], in which the use of a finer space (in h or p) is common.

n	$ \lambda - \lambda_n $	$ \lambda - \lambda_n - \sum_{K \in \mathcal{T}_n} \eta_K $
1	5.030e-02	4.568e-04
2	2.658e-02	5.289e-04
3	1.728e-02	3.880e-04
4	6.080e-04	4.815e-06
5	3.067e-04	4.668e-06
6	1.480e-04	3.620e-06
7	4.596e-06	2.202e-08
8	2.361e-06	2.289e-08
9	1.684e-06	1.837e-08
10	2.363e-08	8.970e-11
11	1.189e-08	8.851e-11
12	3.043e-09	5.453e-11

TABLE 3. Improved accuracy for the eigenvalue $\lambda = 2\pi^2$.

n	$ \lambda - \lambda_n $	$ \lambda - \lambda_n - \sum_{K \in \mathcal{T}_n} \eta_K $
1	4.121e-01	1.011e-02
2	1.825e-01	7.438e-03
3	1.245e-01	5.714e-03
4	2.231e-02	2.144e-04
5	6.655e-03	1.458e-04
6	1.375e-03	1.636e-05
7	1.332e-04	1.385e-06
8	2.480e-05	7.623e-07
9	2.139e-06	1.585e-08
10	1.580e-07	3.547e-10
11	1.998e-08	1.392e-10
12	5.559e-10	5.009e-11

TABLE 4. Improved accuracy for the eigenvalue $\lambda = 5\pi^2$.

Finally, to more fully demonstrate the performance of Algorithm 1, in Table 5 we report, for the first 15 eigenvalues of the Laplace problem: the number of iterations N and degrees of freedom used to reach a precision of at least $1e - 8$, errors and effectivities on the finest mesh, and the total CPU time for the computation (in seconds).

λ	N	DOFs	elements	$ \lambda - \lambda_N $	$\sum_{K \in \mathcal{T}_N} \eta_K$	effectivity	CPU time
19.73920880	12	812	32	3.043e-09	2.989e-09	1.02	9.361
49.34802200	12	2157	86	5.559e-10	5.558e-10	1.00	48.171
49.34802200	11	2611	89	9.955e-10	9.879e-10	1.01	40.131
78.95683520	11	2317	65	1.957e-09	1.845e-09	1.06	44.835
98.69604401	12	3251	104	3.805e-09	3.789e-09	1.00	62.805
98.69604401	13	3400	113	3.540e-09	3.511e-09	1.01	62.850
128.30485721	13	4478	170	6.190e-09	6.207e-09	1.00	56.895
128.30485721	10	6023	216	9.307e-09	9.642e-09	0.97	58.215
167.78327481	13	6176	224	6.988e-09	7.391e-09	0.95	75.974
167.78327481	12	7138	264	7.860e-09	7.846e-09	1.00	81.785
177.65287921	13	7522	281	7.068e-09	7.035e-09	1.00	119.636
197.39208802	13	10036	393	3.443e-09	3.398e-09	1.01	92.153
197.39208802	13	9695	267	3.614e-10	3.669e-10	0.99	153.207
246.74011002	12	8478	270	2.656e-09	2.838e-09	0.94	119.962
246.74011002	12	11606	387	3.723e-09	4.027e-09	0.92	159.485

TABLE 5. Results for the hp -adaptive on the first 15 eigenvalues for the Laplace problem on the unit square.

5.2. **The L-Shaped Domain.** A standard simple example for which (some of) the eigenvalues and eigenfunctions are not explicitly known, and the eigenfunctions have reduced regularity, $u \notin H^2$, is provided by the L-shaped domain

$$\Omega = [0, 1]^2 \setminus ([0.5, 1] \times [0, 0.5]) ,$$

for which we again consider (5.1). The re-entrant corner at $(0.5, 0.5)$ causes some of the eigenfunctions to be singular there. This is certainly the case for the eigenfunctions associated with the smallest eigenvalue. The theory given in Section 3 does not cover such cases.

In Table 6 we have used Algorithm 1 to compute the first eigenvalue. The main difference between Table 6 and Table 1 (our analogous results for the unit square) is the fact that the effectivity index is in this case not close to 1, due to the singularity in the gradient of the first eigenfunction. Because of this, the auxiliary space \tilde{S}_n constructed by DualSpace is not “fine” enough for computing an approximation of z which is sufficient for estimating the error for eigenvalues to such a high level of accuracy. In this case the exact value of the eigenvalue is unknown, so in order to be able to compute the effectivity index, we use as a reference value, the eigenvalue computed at a very fine level. Despite this loss in effectivity, we see in Figure 2 that the convergence rate is still exponential. In Figure 3 we depict the final mesh with different colors to indicate different orders of polynomials. Unsurprisingly the elements are very small around the reentering corner, where the singularity sits and the orders of polynomials increase moving away from the singularity. The primary reason for including this example is to demonstrate that Algorithm 2 may be necessary in order to obtain effectivities near 1, and that this goal can in fact be achieved by using this variant. In Table 7 we have used Algorithm 2 with $m = 2$ to compute the first eigenvalue of the problem on the L-shaped domain. As can be seen the effectivity index is very close to 1 again, as in case of smooth problems. Comparing Table 7 with Table 6 it is clear that the difference

in the construction of the dual space has almost no effect on the convergence rate of the method, but just on the effectivity index. In Table 8 we compare the true error $|\lambda - \lambda_n|$ with the error for the improved estimation for the eigenvalue $\lambda_n + \sum_{K \in \mathcal{T}_n} \eta_K$, based on Algorithm 2, where we again see an increase by one or two orders of magnitude.

n	DOFs	elements	$ \lambda - \lambda_n $	$\sum_{K \in \mathcal{T}_n} \eta_K$	effectivity
1	108	12	1.748e-01	1.847e-01	0.95
2	189	21	1.019e-01	1.087e-01	0.94
3	284	30	7.600e-02	7.003e-02	1.09
4	425	39	3.096e-02	2.480e-02	1.25
5	616	45	1.464e-02	9.804e-03	1.49
6	902	45	7.641e-03	3.995e-03	1.91
7	1339	45	4.903e-03	2.131e-03	2.30
8	2320	54	1.945e-03	8.446e-04	2.30
9	3078	63	7.718e-04	3.352e-04	2.30
10	4039	72	3.063e-04	1.330e-04	2.30
11	4971	81	1.215e-04	5.280e-05	2.30
12	5941	90	4.823e-05	2.095e-05	2.30
13	7100	99	1.914e-05	8.315e-06	2.30
14	8684	108	7.596e-06	3.300e-06	2.30
15	10268	117	3.014e-06	1.310e-06	2.30
16	12425	126	1.195e-06	5.198e-07	2.30

TABLE 6. Results for the hp -adaptive method on the first eigenvalue of the L-shape domain.

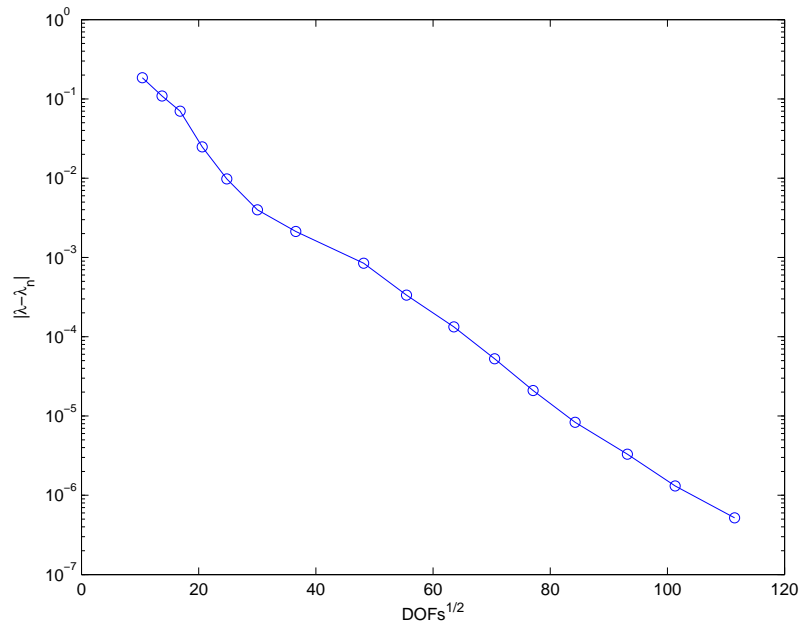


FIGURE 2. Convergence for first eigenvalue of the L-shape domain.

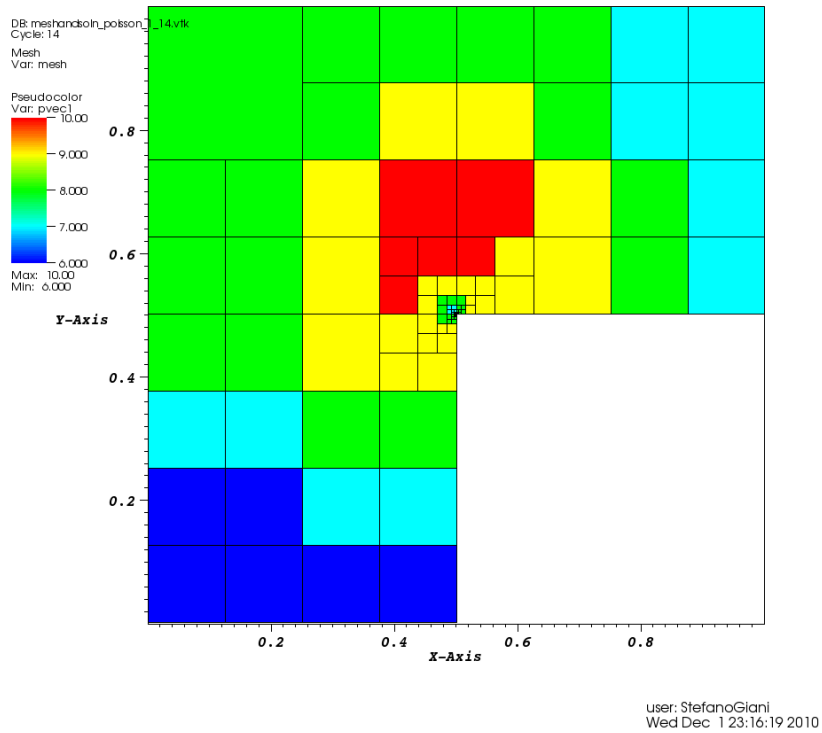


FIGURE 3. *hp*-adapted mesh for the L-shape domain.

n	DOFs	elements	$ \lambda - \lambda_n $	$\sum_{K \in \mathcal{T}_n} \eta_K$	effectivity
1	108	12	1.748e-01	2.072e-01	0.84
2	189	21	1.019e-01	1.158e-01	0.88
3	284	30	7.600e-02	8.084e-02	0.94
4	425	39	3.096e-02	2.983e-02	1.04
5	616	45	1.464e-02	1.276e-02	1.15
6	902	45	7.641e-03	7.455e-03	1.02
7	1339	45	4.903e-03	4.642e-03	1.06
8	2045	54	1.945e-03	1.841e-03	1.06
9	2688	63	7.718e-04	7.306e-04	1.06
10	3437	72	3.063e-04	2.899e-04	1.06
11	4411	81	1.215e-04	1.151e-04	1.06
12	5434	90	4.823e-05	4.566e-05	1.06
13	6575	99	1.914e-05	1.812e-05	1.06
14	7862	108	7.596e-06	7.192e-06	1.06
15	9670	117	3.014e-06	2.854e-06	1.06
16	11548	126	1.195e-06	1.133e-06	1.06

TABLE 7. Results for the hp -adaptive method on the first eigenvalue of the L-shape domain using Algorithm 2.

n	$ \lambda - \lambda_n $	$ \lambda - \lambda_n - \sum_{K \in \mathcal{T}_n} \eta_K $
1	1.748e-01	3.240e-02
2	1.019e-01	1.386e-02
3	7.600e-02	4.845e-03
4	3.096e-02	1.135e-03
5	1.464e-02	1.876e-03
6	7.641e-03	1.856e-04
7	4.903e-03	2.612e-04
8	1.945e-03	1.037e-04
9	7.718e-04	4.116e-05
10	3.063e-04	1.633e-05
11	1.215e-04	6.481e-06
12	4.823e-05	2.571e-06
13	1.914e-05	1.020e-06
14	7.596e-06	4.041e-07
15	3.014e-06	1.597e-07
16	1.195e-06	6.278e-08

TABLE 8. Improved accuracy for the first eigenvalue of the L-shaped domain.

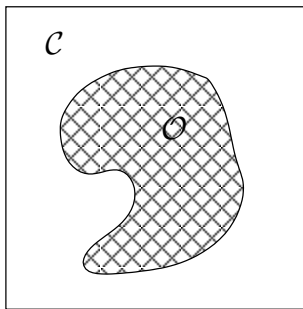


FIGURE 4. A generic composite two phased material.

5.3. Problems with a large coupling limit. As a first class of benchmark problems we consider the perturbation of the free Hamiltonian by a singular step potential, cf. Figure 4. The eigenvalue problem can be formulated as

$$(5.2) \quad \mathbf{A}_\kappa^{\mathcal{O}} \psi := -\Delta \psi + \kappa \chi_{\mathcal{O}} \cdot \psi = \lambda \psi,$$

$$(5.3) \quad \psi \in H_0^1(\Omega), \|\psi\|_0 = 1.$$

Here $\Omega \subset \mathbb{R}^2$ is bounded, connected and open, and $\chi_{\mathcal{O}}$ is the characteristic function of the set $\mathcal{O} \subset \Omega$. Alternatively we can set $\mathcal{C} = \Omega \setminus \mathcal{O}$ and study the problem

$$(5.4) \quad \mathbf{A}_\kappa^{\mathcal{C}} \psi := -\Delta \psi + \kappa \chi_{\mathcal{C}} \cdot \psi = \lambda \psi,$$

$$(5.5) \quad \psi \in H_0^1(\Omega), \|\psi\|_0 = 1.$$

The second problem models a waveguide type problem, whereas the first is characteristic of the hard-core scattering problems. Furthermore, such short range potentials appear frequently in the study of the spectral properties of disordered media [8, 10, 17, 41]. Similarly formulated problems appear also in the study of optical wave-guides and other nano-devices (see [11, 33]). For any given $\kappa > 0$, the eigenvalue problems (5.2) and (5.4) are of the sort considered in [21], where convergence of several adaptive methods for eigenvalue problems was proved. A third type of problem, for which the jump discontinuity is in the derivative, will also be discussed below. Analyzing and understanding the spectra of such problems is a key ingredient in the inverse spectral theory behind nondestructive sensing methods described in [1, 2].

Remark 5.1. If Ω is convex and $\mathcal{O} \subset \Omega$ is measurable, then all eigenfunctions ψ associated with eigenvalue problems of the form

$$-\Delta \psi + \kappa \chi_{\mathcal{O}} \cdot \psi = \lambda \psi, \quad \psi \in H_0^1(\Omega), \quad \|\psi\|_0 = 1$$

are in $H_{\mathcal{A}}^2 = H^2(\Omega)$. In particular, this holds for problems (5.2) and (5.4) in this subsection, as well as for problems (5.10) and (5.12) in Subsection 5.4. This fact is apparent from well-known regularity theory for boundary value problems when one notes that $-\Delta \psi = (\lambda - \kappa \chi_{\mathcal{O}}) \psi \in L^2(\Omega)$.

For the simulations described in Tables 9-10, we set $\Omega = [-2, 2]^2$, $\mathcal{O} = [-1, 1]^2$ and $\kappa = 1$. In both cases, Algorithm 1 is used, and since the true eigenvalues are not known, we stop when the error estimator $|\sum_{K \in \mathcal{T}_n} \eta_K|$ goes below $1e - 10$.

λ	N	DOFs	elements	CPU time
1.87133388216	13	5024	40	40.229
3.46969764021	14	4537	58	31.103
3.46969764021	16	5420	64	49.315
5.17025007350	16	6576	64	83.026
6.37878411287	14	21796	1102	95.810
6.60864815270	15	8226	115	85.369
8.20584707564	15	8771	160	72.428
8.20584707564	16	11282	157	98.820
10.90836153911	17	14041	172	341.247
10.90836153911	18	14920	256	240.053

TABLE 9. Results for the hp -adaptive on the first 10 eigenvalues of (5.2) with $\kappa = 1$.

λ	N	DOFs	elements	CPU time
1.53507937290	27	2304	16	48.785
3.65052961461	15	4752	70	17.924
3.65052961463	16	5208	64	46.037
5.66897040432	15	6500	64	79.265
6.75875052154	16	10358	124	89.592
6.93592873731	14	17758	886	79.887
8.81189701874	15	10380	145	65.724
8.81189701882	15	11060	148	72.855
11.09179175102	15	10834	190	128.062
11.09179175102	20	19775	196	313.822

TABLE 10. Results for the hp -adaptive on the first 10 eigenvalues of (5.4) with $\kappa = 1$.

A second type of problem considered here has its jump discontinuity on the second-derivative term, and is given formally by,

$$(5.6) \quad \mathbb{T}_\kappa \psi := -\nabla \cdot [(1 + \kappa \chi_{\mathcal{C}}) \nabla] \psi = \lambda \psi,$$

$$(5.7) \quad \psi \in H_0^1(\Omega), \|\psi\|_{H^0} = 1.$$

As a test example, we consider $\Omega = (-1, 1)^2$ with $\mathcal{C} = (-1, 1) \times (0, 1)$. The structure of the domain and differential operator is such that the eigenvalues and eigenfunctions may be computed by (partially) analytic means. In particular, using separation-of-variables and continuity of both the eigenfunction and its flux across the interface between \mathcal{C} and its complement, we deduce that all eigenfunctions are in $H_{\mathcal{A}}^2(\Omega)$, and the eigenvalues are of one of two types:

I) For $m \in \mathbb{N}$ and $\lambda \in (\frac{\pi^2 m}{4}, (1 + \kappa) \frac{\pi^2 m}{4})$, we define

$$K_m = \sqrt{\lambda - \frac{\pi^2 m}{4}} \quad , \quad L_m = \sqrt{\frac{\pi^2 m}{4} - \frac{\lambda}{1 + \kappa}} .$$

Any admissible λ which satisfies

$$(1 + \kappa)L_n \cosh L_n \sin K_n + K_n \cos K_n \sinh L_n = 0$$

is an eigenvalue of \mathbb{T}_κ .

II) For $m \in \mathbb{N}$ and $\lambda > (1 + \kappa)\frac{\pi^2 m}{4}$, we define K_m as before, and

$$M_m = \sqrt{\frac{\lambda}{1 + \kappa} - \frac{\pi^2 m}{4}}.$$

Any admissible λ which satisfies

$$(1 + \kappa)M_n \cos M_n \sin K_n + K_n \cos K_n \sin M_n = 0$$

is an eigenvalue of \mathbb{T}_κ .

Choosing m and κ , these equations can be solved with extremely high accuracy and precision using a computer algebra system. In Table 11 we provide data for the first 10 eigenvalues of (5.6) for $\kappa = 9$, using Algorithm 1 and stopping when the error estimator $|\sum_{K \in \mathcal{T}_n} \eta_K|$ goes below $1e - 10$. We include the exact eigenvalues to full 16-digit accuracy (rounded) together with our computed approximations at termination of the algorithm. As is apparent, each of the computed eigenvalues is accurate to (at least) 10 digits.

Exact λ	Type , m	λ	N	DOFs	elements	CPU time
11.09406656702782	I , 1	11.09406656703	11	2346	40	3.376
19.08195563003389	I , 2	19.08195563004	12	3578	58	18.855
31.63979194296281	I , 3	31.63979194297	12	8136	121	73.763
33.74934000401159	II , 2	33.74934000407	12	5431	82	50.995
46.23920055155409	I , 2	46.23920055158	15	10792	154	217.012
49.02100175422781	I , 4	49.02100175426	16	13510	256	185.309
56.65491310722691	II , 1	56.65491310728	15	13723	169	422.041
59.81053365500185	I , 3	59.81053365509	14	9455	166	109.665
71.29286859201738	I , 5	71.29286859203	23	58442	325	533.272
77.59668562450120	I , 4	77.59668562455	20	31443	256	487.148

TABLE 11. Results for the hp -adaptive on the first 10 eigenvalues of (5.6) with $\kappa = 9$.

5.3.1. *A computational study of the large coupling limit.* We finally turn to examples which give this subsection its name—those for which we investigate the asymptotic behavior of the spectra of the operators \mathbf{A}_κ^C and \mathbb{T}_κ^C as $\kappa \rightarrow \infty$. To this end let $\lambda_1^\kappa \leq \lambda_2^\kappa \leq \dots$ and $\mu_1^\kappa \leq \mu_2^\kappa \leq \dots$ be the ordered eigenvalues of the operators \mathbf{A}_κ^C and \mathbb{T}_κ^C , respectively, counted according to multiplicity. Furthermore, let $\lambda_1^\infty \leq \lambda_2^\infty \leq \dots$ denote the eigenvalues of the limit operator \mathbf{A}_∞ , which is, in both cases, defined by

$$(5.8) \quad \mathbf{A}_\infty \psi = -\Delta \psi = \lambda \psi,$$

$$(5.9) \quad \psi \in H_0^1(\mathcal{O}), \|\psi\|_{H_0^1} = 1.$$

According to the theory from [8, 11, 17, 23, 38] $\lambda_i^\kappa \rightarrow \lambda_i^\infty$ and $\mu_i^\kappa \rightarrow \lambda_i^\infty$ as $\kappa \rightarrow \infty$. The difference is in the convergence rates. According to [23] we have

$$\frac{|\mu_i^\kappa - \lambda_i^\infty|}{\lambda_i^\infty} = O(\kappa^{-1}), \quad i \in \mathbb{N}$$

for any problem of the type (5.6), but for problems of the type (5.4) we have

$$\frac{|\lambda_i^\kappa - \lambda_i^\infty|}{\lambda_i^\infty} = O(\kappa^{-\alpha}), \quad i \in \mathbb{N}$$

for some $\alpha \in (0, 1]$. The parameter α depends on the regularity properties of the boundary $\partial\mathcal{O}$. This analysis is much more involved (cf. [26]), and we consider it empirically in Table 12 for the first eigenvalue of (5.4). In Table 12-(a) we estimate the value of α for the first eigenvalue of problem (5.6) for a sequence of values of κ , recalling that, for problem (5.6), $\lambda_1^\infty = \pi^2 + (\pi/2)^2$. In Table 12-(b) we estimate the value of α for the first eigenvalue of problem (5.4) for a sequence of values of κ , we recalling that, for problem (5.4), $\lambda_1^\infty = 2\pi^2$.

κ	α	κ	α
1.0e+01	-	1.0e+01	-
1.0e+02	0.950	1.0e+02	0.276
1.0e+03	0.996	1.0e+03	0.447
1.0e+04	1.000	1.0e+04	0.486
1.0e+05	1.000	1.0e+05	0.496
1.0e+06	1.000	1.0e+06	0.499
1.0e+07	1.000	1.0e+07	0.500
1.0e+08	1.000	1.0e+08	0.500

(a)
(b)

TABLE 12. Estimations for the exponent α for problem (5.6) and for the problem for problem (5.4).

5.4. Benchmarking the adaptivity of eigenvalue methods. Two key constants related to the quality of *a posteriori* error estimates for eigenvalue problems are

- (1) The stability constant C_{stb} , measuring the distance to the unwanted component of the spectrum.
- (2) The regularity constant C_{reg} , measuring the regularity properties of the eigenfunctions.

In our basic estimator result from Corollary 3.3 the stability constants are implicit in the assumption that the dual problem is well-posed and the assumption that we need H_A^2 regularity to establish rigorous convergence results. In this section we present two parameter dependent examples where either H_A^2 regularity is violated or the eigenvalue clustering is increased as a controlled function of the problem parameter. This gives us an opportunity to both generate an interesting benchmark—e.g. one which is close to violating either the requirement (1) or (2) in a controlled way—and to use the analytical knowledge of the spectral behavior of the eigenvalues in the parameter limit in order to circumstantially validate the method.

For a discussion of the roll played by these constants in eigenvalue estimates see [34, 5]. The reference [5] is particularly interesting as a motivation for providing accurate benchmark eigenvalues for use in experimental studies and for gaining insight in situations where one does not have an analytical option. We have illustrated a potential of our method in this experimental context in Section 5.3.1 and will do so again for the following two problems.

5.4.1. *Problems with an asymptotic doubling of the multiplicity.* As a prototype example in this class we consider the family of problems

$$(5.10) \quad -\Delta\psi + \kappa V_{MD} \cdot \psi = \lambda\psi,$$

$$(5.11) \quad \psi \in H_0^1([-1, 1]^2), \|\psi\|_0 = 1.$$

where the function V_{MD} is defined as the characteristic function of the coalescent squares which are denoted by \mathcal{M}_1 in Figure 5. This example was originally proposed and solved as a test example for an eigenvalue problem un electromagnetism by M. Dauge in [16]. In its original formulation the problem is much more challenging, since the jumps are contained in the second order term, cf. [16]. A similar problem — having jumps in the second order term — has also been studied as an interesting example in the context of ill-posed boundary value problems by Knyazev and Widlund in [32]. There, an extensive regularity theory for such problems is presented as well.

In Table 13 we provide data for the first 10 eigenvalues of (5.10) with $\kappa = 1$ using Algorithm 1. Again, the exact eigenvalues for this problem eigenvalues are not known, so we stop when the $|\sum_{K \in \mathcal{T}_n} \eta_K|$ goes below $1e - 10$.

λ	N	DOFs	elements	CPU time
5.42471651467	13	2028	16	13.061
12.47333477067	15	9121	445	23.624
13.19367701575	14	8155	391	18.367
20.22822122972	13	2512	64	7.400
25.16706773416	15	24075	1162	63.759
25.18999056233	15	6521	112	38.258
32.43757892927	14	19757	862	49.056
32.69700326366	14	18810	865	45.874
42.39525913789	18	62361	904	352.948
42.51072321200	19	67045	862	302.182

TABLE 13. Results for the hp -adaptive on the first 10 eigenvalues of (5.10) with $\kappa = 1$.

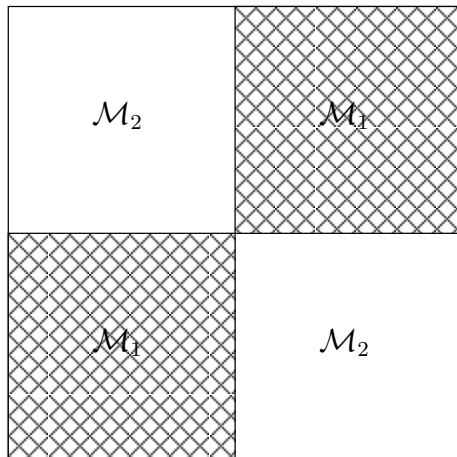


FIGURE 5. A modification of the touching squares example of M. Dauge. The potential V_{MD} is the characteristic function of the coalescent squares denoted by V_{MD} .

According to the theory from [8, 11, 17, 23, 38], as $\kappa \rightarrow \infty$ we have that the smallest two eigenvalues of (5.10), λ_1^κ and λ_2^κ , with are distinct for any finite κ , both converge to the double eigenvalue $2\pi^2$ of the Dirichlet Laplace eigenvalue problem posed in the domain consisting of the two unit squares labelled \mathcal{M}_2 in Figure 5. Additionally, it holds that

$$\frac{|\lambda_1^\kappa - 2\pi^2|}{2\pi^2} = O(\kappa^{-\alpha}), \quad \frac{|\lambda_2^\kappa - 2\pi^2|}{2\pi^2} = O(\kappa^{-\alpha}) .$$

We will estimate $0 < \alpha \leq 1$ by fitting the computed error estimates. Furthermore, this will serve as an indirect check of our accuracy claims. The theory from [11] does not cover this case, but we formally expect that $\alpha = 1/2$. In Table 14-(a) and Table 14-(b) we give our estimated values of α for the first two eigenvalues of problem (5.10) for a sequence of values of κ .

κ	α	κ	α
1.0e+01	-	1.0e+01	-
1.0e+02	0.469	1.0e+02	0.276
1.0e+03	0.486	1.0e+03	0.447
1.0e+04	0.488	1.0e+04	0.486
1.0e+05	0.496	1.0e+05	0.496
1.0e+06	0.499	1.0e+06	0.499
1.0e+07	0.500	1.0e+07	0.500
		1.0e+08	0.500

(a)
(b)

TABLE 14. Estimations for the exponent α for the first eigenvalue of (5.10) and for the second eigenvalue.

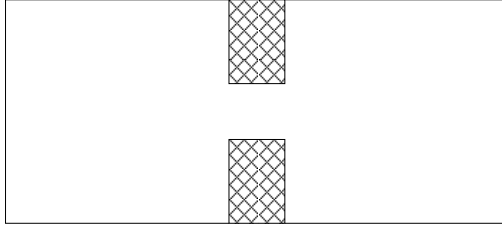


FIGURE 6. A dumbbell example. The region \mathcal{C} is shaded.

5.4.2. *Problems with an asymptotic loss of H_A^2 regularity.* We consider the problem

$$(5.12) \quad -\Delta\psi + \kappa\chi_{\mathcal{C}} \cdot \psi = \lambda\psi,$$

$$(5.13) \quad \psi \in H_0^1(\Omega), \|\psi\|_0 = 1.$$

where Ω is the rectangular domain pictured in Figure 6, and \mathcal{C} is the shaded region. In the limit as $\kappa \rightarrow \infty$ we obtain the dumbbell example from [9], where the domain consists of two $\pi \times \pi$ squares coupled by a $\frac{\pi}{4} \times \frac{\pi}{4}$ square ‘‘bridge’’. In Table 15 we provide data for the first 10 eigenvalues of (5.12) with $\kappa = 1$, using Algorithm 1. Moreover, in Table 16 we show the convergence of the first 10 eigenvalues of (5.12) to the limit problem as $\kappa \rightarrow \infty$. The quantities β_i are defined as

$$\beta_i := \frac{|\lambda_i - \lambda_i^\infty|}{\lambda_i^\infty},$$

where $\lambda_i = \lambda_i^\kappa$ are the eigenvalues of (5.12) and λ_i^∞ are the corresponding eigenvalues of the Dirichlet Laplacian on the dumbbell domain, ordered according to multiplicity. Also, in Table 17 we give estimates of the rate of convergence of the first 10 eigenvalues, where

$$\beta_i = O(\kappa^{-\alpha_i}).$$

We note that the eigenfunction(s) of (5.12) associated with $\lambda_i = \lambda_i^\kappa$ are in H_A^2 for all i and all (finite) κ ; but the eigenfunction(s) of the Dirichlet Laplacian on the dumbbell domain associated with λ_i^∞ are generally not in H_A^2 .

λ	N	DOFs	elements	CPU time
2.41912769822	15	5121	36	65.504
5.55688992939	19	3414	36	40.281
5.95612871083	20	3338	36	39.784
8.92506550331	18	3475	36	43.135
11.01367309016	17	6288	168	54.525
11.45047929172	16	6800	216	41.064
14.38062704740	17	5288	144	41.048
14.53086734821	17	5288	144	37.072
18.79848740656	19	9471	156	28.084
19.00148186721	19	9181	144	160.707

TABLE 15. Results for the hp -adaptive on the first 10 eigenvalues of (5.12) with $\kappa = 1$.

κ	β_1	β_2	β_3	β_4	β_5	β_6	β_7	β_8	β_9	β_{10}
1.0e+00	0.687	0.350	0.572	0.359	0.230	0.353	0.271	0.414	0.287	0.281
1.0e+01	0.521	0.293	0.368	0.287	0.206	0.160	0.234	0.301	0.242	0.175
1.0e+02	0.240	0.153	0.132	0.129	0.124	0.072	0.073	0.081	0.093	0.073
1.0e+03	0.087	0.058	0.045	0.045	0.050	0.028	0.025	0.029	0.029	0.026
1.0e+04	0.029	0.020	0.015	0.015	0.017	0.009	0.008	0.010	0.009	0.009
1.0e+05	0.009	0.006	0.005	0.005	0.006	0.003	0.003	0.003	0.003	0.003
1.0e+06	0.003	0.002	0.002	0.002	0.002	0.001	0.001	0.001	0.001	0.001

TABLE 16. Convergence of the first 10 eigenvalues of (5.12) to those of the dumbbell problem as κ increases.

κ	α_1	α_2	α_3	α_4	α_5	α_6	α_7	α_8	α_9	α_{10}
1.0e+00	-	-	-	-	-	-	-	-	-	-
1.0e+01	0.121	0.077	0.192	0.098	0.048	0.345	0.065	0.139	0.075	0.207
1.0e+02	0.336	0.283	0.445	0.346	0.221	0.343	0.507	0.568	0.417	0.381
1.0e+03	0.440	0.422	0.463	0.457	0.396	0.417	0.459	0.453	0.508	0.446
1.0e+04	0.477	0.470	0.485	0.484	0.465	0.472	0.480	0.477	0.492	0.481
1.0e+05	0.490	0.488	0.494	0.494	0.489	0.491	0.493	0.491	0.495	0.492
1.0e+06	0.495	0.494	0.497	0.497	0.496	0.497	0.498	0.496	0.497	0.496

TABLE 17. Rate of convergence of the first 10 eigenvalues of (5.12) to those of the dumbbell problem as κ increases.

ACKNOWLEDGEMENT

L. G. was supported by the grant: “Spectral decompositions – numerical methods and applications”, Grant Nr. 037-0372783-2750 of the Croatian MZOS.

We would like to thanks Paul Houston and Edward Hall for kind support and very useful discussions.

REFERENCES

- [1] H. Ammari, Y. Capdeboscq, H. Kang, and A. Kozhemyak. Mathematical models and reconstruction methods in magneto-acoustic imaging. *European J. Appl. Math.*, 20(3):303–317, 2009.
- [2] H. Ammari, H. Kang, E. Kim, and H. Lee. Vibration testing for anomaly detection. *Math. Methods Appl. Sci.*, 32(7):863–874, 2009.
- [3] H. Ammari, H. Kang, and H. Lee. Asymptotic analysis of high-contrast phononic crystals and a criterion for the band-gap opening. *Arch. Ration. Mech. Anal.*, 193(3):679–714, 2009.
- [4] D. Arnold, F. Brezzi, B. Cockburn, and L. Marini. Unified analysis of discontinuous galerkin methods for elliptic problems. *SIAM J. Numer. Anal.*, 24(3):1749–1779, 2001.
- [5] L. Banjai, S. Börm, and S. Sauter. FEM for elliptic eigenvalue problems: how coarse can the coarsest mesh be chosen? An experimental study. *Comput. Vis. Sci.*, 11(4-6):363–372, 2008.
- [6] R. Bank, L. Grubišić, and J. S. Owall. A framework for robust eigenvalue and eigenvector error estimation and ritz value convergence enhancement. *MPI-MSI Preprint 42*, 2010.
- [7] R. Becker and R. Rannacher. An optimal control approach to a posteriori error estimation in finite element methods. *Acta Numer.*, 10:1–102, 2001.

- [8] A. Ben Amor and J. F. Brasche. Sharp estimates for large coupling convergence with applications to Dirichlet operators. *J. Funct. Anal.*, 254(2):454–475, 2008.
- [9] T. Betcke and L. N. Trefethen. Reviving the method of particular solutions. *SIAM Rev.*, 47(3):469–491 (electronic), 2005.
- [10] J. F. Brasche, R. Figari, and A. Teta. Singular Schrödinger operators as limits of point interaction Hamiltonians. *Potential Anal.*, 8(2):163–178, 1998.
- [11] V. Bruneau and G. Carbou. Spectral asymptotic in the large coupling limit. *Asymptot. Anal.*, 29(2):91–113, 2002.
- [12] L.-Q. Cao and J.-Z. Cui. Asymptotic expansions and numerical algorithms of eigenvalues and eigenfunctions of the Dirichlet problem for second order elliptic equations in perforated domains. *Numer. Math.*, 96(3):525–581, 2004.
- [13] L.-Q. Cao and J.-L. Luo. Multiscale numerical algorithm for the elliptic eigenvalue problem with the mixed boundary in perforated domains. *Appl. Numer. Math.*, 58(9):1349–1374, 2008.
- [14] A. Cliffe, E. Hall, P. Houston, E. T. Phipps, and A. G. Salinger. Adaptivity and a posteriori error control for bifurcation problems ii: Incompressible fluid flow in open systems with z_2 symmetry. *Journal of Scientific Computing*, (submitted). URL: <http://eprints.nottingham.ac.uk/1257/>.
- [15] K. A. Cliffe, E. J. Hall, and P. Houston. Adaptive discontinuous Galerkin methods for eigenvalue problems arising in incompressible fluid flows. *SIAM J. Sci. Comput.*, 31(6):4607–4632, 2009/10.
- [16] M. Dauge. Benchmark collection, retrieved on March 31st 2010. URL: <http://perso.univ-rennes1.fr/monique.dauge/benchmax.html>.
- [17] M. Demuth, F. Jeske, and W. Kirsch. Quantitative estimates for Schrödinger and Dirichlet semigroups. In *Journées “Équations aux Dérivées Partielles” (Saint-Jean-de-Monts, 1992)*, pages Exp. No. XVII, 6. École Polytech., Palaiseau, 1992.
- [18] M. Demuth and M. Krishna. *Determining spectra in quantum theory*, volume 44 of *Progress in Mathematical Physics*. Birkhäuser Boston Inc., Boston, MA, 2005.
- [19] T. Eibner and J. Melenk. An adaptive strategy for hp-fem based on testing for analyticity. *Comp. Mech.*, 39:575–595, 2007.
- [20] A. Ern, A. F. Stephansen, and P. Zunino. A discontinuous Galerkin method with weighted averages for advection-diffusion equations with locally small and anisotropic diffusivity. *IMA J. Numer. Anal.*, 29(2):235–256, 2009.
- [21] E. M. Garau, P. Morin, and C. Zuppa. Convergence of adaptive finite element methods for eigenvalue problems. *Math. Models Methods Appl. Sci.*, 19(5):721–747, 2009.
- [22] S. Giani and P. Houston. *ADIGMA - A European Initiative on the Development of Adaptive Higher-Order Variational Methods for Aerospace Applications*, chapter 28, pages 399–411. Springer, 2010.
- [23] L. Grubišić. Relative convergence estimates for the spectral asymptotic in the large coupling limit. *Integral Equations Operator Theory*, 65(1):51–81, 2009.
- [24] R. Hartmann and P. Houston. Adaptive discontinuous Galerkin finite element methods for nonlinear hyperbolic conservation laws. *SIAM J. Sci. Comput.*, 24(3):979–1004, 2002.
- [25] R. Hartmann and P. Houston. An optimal order interior penalty discontinuous Galerkin discretization of the compressible Navier–Stokes equations. *J. Comp. Phys.*, 227:9670–9685, 2008.
- [26] R. Hempel and O. Post. Spectral gaps for periodic elliptic operators with high contrast: an overview. In *Progress in analysis, Vol. I, II (Berlin, 2001)*, pages 577–587. World Sci. Publ., River Edge, NJ, 2003.
- [27] P. D. Hislop and O. Post. Anderson localization for radial tree-like quantum graphs. *Waves Random Complex Media*, 19(2):216–261, 2009.
- [28] P. Houston, D. Schötzau, and T. Wihler. Energy norm a posteriori error estimation of hp-adaptive discontinuous Galerkin methods for elliptic problems. *Math. Mod. Meth. Appl. Sci.*, 17(1):33–62, 2007.
- [29] P. Houston, C. Schwab, and E. Süli. Discontinuous hp-finite element methods for advection-diffusion-reaction problems. *SIAM J. Numer. Anal.*, 39(6):2133–2163, 2002.
- [30] P. Houston and E. Süli. A note on the design of hp-adaptive finite element methods for elliptic partial differential equations. *Comput. Methods Appl. Mech. Engrg.*, 194(2-5):229–243, 2005.
- [31] T. Kato. *Perturbation theory for linear operators*. Classics in Mathematics. Springer-Verlag, Berlin, 1995. Reprint of the 1980 edition.

- [32] A. Knyazev and O. Widlund. Lavrentiev regularization + Ritz approximation = uniform finite element error estimates for differential equations with rough coefficients. *Math. Comp.*, 72(241):17–40 (electronic), 2003.
- [33] T. Koprucki, R. Eymard, and J. Fuhrmann. Convergence of a finite volume scheme to the eigenvalues of a schroedinger operator. Technical report, WIAS Preprint No. 1260, 2007.
- [34] M. G. Larson. A posteriori and a priori error analysis for finite element approximations of self-adjoint elliptic eigenvalue problems. *SIAM J. Numer. Anal.*, 38(2):608–625 (electronic), 2000.
- [35] A. Naga, Z. Zhang, and A. Zhou. Enhancing eigenvalue approximation by gradient recovery. *SIAM J. Sci. Comput.*, 28(4):1289–1300 (electronic), 2006.
- [36] I. Perugia and D. Schötzau. The hp -local discontinuous Galerkin method for low-frequency time-harmonic Maxwell equations. *Math. Comp.*, 72(243):1179–1214, 2003.
- [37] M. R. Racheva and A. B. Andreev. Superconvergence postprocessing for eigenvalues. *Comput. Methods Appl. Math.*, 2(2):171–185, 2002.
- [38] E. Sánchez-Palencia. Asymptotic and spectral properties of a class of singular-stiff problems. *J. Math. Pures Appl. (9)*, 71(5):379–406, 1992.
- [39] S. Sauter. hp -finite elements for elliptic eigenvalue problems: error estimates which are explicit with respect to λ , h , and p . *SIAM J. Numer. Anal.*, 48(1):95–108, 2010.
- [40] D. Schötzau and L. Zhu. A robust a-posteriori error estimator for discontinuous galerkin methods for convection-diffusion equations. *Appl. Numer. Math.*, 59:2236–2255, 2009.
- [41] P. Stollmann. *Caught by disorder*, volume 20 of *Progress in Mathematical Physics*. Birkhäuser Boston Inc., Boston, MA, 2001. Bound states in random media.
- [42] J. Xu and A. Zhou. A two-grid discretization scheme for eigenvalue problems. *Math. of Comput.*, 70(233):17–25, 2001.
- [43] L. Zhu, S. Giani, P. Houston, and D. Schötzau. Energy norm a-posteriori error estimation for hp -adaptive discontinuous galerkin methods for elliptic problems in three dimensions. *Math. Models Methods Appl. Sci.*, (to appear), 2011.

SCHOOL OF MATHEMATICAL SCIENCES UNIVERSITY OF NOTTINGHAM , UNIVERSITY PARK, NOTTINGHAM, NG7 2RD, UNITED KINGDOM

E-mail address: stefano.giani@nottingham.ac.uk

UNIVERSITY OF ZAGREB, DEPARTMENT OF MATHEMATICS, BIJENIČKA 30, 10000 ZAGREB, CROATIA

E-mail address: luka.grubisic@math.hr

UNIVERSITY OF KENTUCKY, DEPARTMENT OF MATHEMATICS, PATTERSON OFFICE TOWER 761, LEXINGTON, KY 40506-0027, USA

E-mail address: jovall@ms.uky.edu